

## MEASUREMENTS OF HEATING AT STREAM-STREAM INTERACTIONS

L. Jian<sup>1</sup>, C. T. Russell<sup>1</sup>, J. T. Gosling<sup>2</sup>, and J. G. Luhmann<sup>3</sup>

<sup>1</sup>*Institute of Geophysics and Planetary Physics, University of California Los Angeles, CA 90095-1567, USA  
(ljan@igpp.ucla.edu) (ctrussell@igpp.ucla.edu)*

<sup>2</sup>*LASP, University of Colorado, 1234 Innovation Drive, Boulder, CO, 80303, USA (jack.gosling@lasp.colorado.edu)*

<sup>3</sup>*Space Sciences Laboratory, University of California Berkeley, Space Sciences Laboratory, Berkeley, CA 94720-7450  
(jgluhman@ssl.berkeley.edu)*

### ABSTRACT

Both adiabatic and non-adiabatic heating occurs when solar wind streams collide. Between the streams a ridge of pressure arises that compressionally heats the plasma. Eventually the pressure ridge develops a forward-reverse shock pair that leads to further heating. In order to characterize the strength of the interaction between streams and identify the presence or absence of shocks, we use the total perpendicular pressure (thermal plus magnetic). The height of the pressure maximum indicates the strength of the interaction. This strength varies about a factor of two over the solar cycle. Shocks or shock-like jumps in pressure are surprisingly frequent, appearing in about 38% of the stream interactions from 1995 to 2003. At one AU it is clear from the duration and strength of the heated plasma behind the shocks that the shocks have only recently formed.

### 1. INTRODUCTION

The magnetic structure of the corona controls solar wind velocity. For much of the solar cycle the magnetic field in the corona, well above the photosphere, is roughly that of a dipole tilted with respect to the rotation axis of the Sun. As the solar magnetic field evolves through the 11-year solar activity cycle, this tilt varies, producing the change in the configuration of heliospheric current sheet. The dipole tends to be nearly aligned with the rotation axis near solar activity minimum (e.g., Hundhausen, 1997), whereas it tends to be inclined substantially relative to the solar rotation axis on the declining phase of the solar cycle. Near solar activity maximum the solar magnetic field is sufficiently complex that the dipole approximation is not useful (e.g., Gosling and Pizzo, 1999).

The fast solar wind originates principally from high heliolatitudinal coronal holes, while the slow solar wind arises near the heliospheric current sheet. Since these radially aligned parcels of plasma originate from different positions on the Sun at different times, they are threaded by different magnetic field lines and are thus prevented from interpenetrating (Gosling and Pizzo, 1999). When they move away from the Sun, the faster wind runs into slower wind ahead while simultaneously outrunning slower trailing wind as indicated in Fig. 1. A compression forms on the rising-speed portion of a high-speed stream, and a rarefaction forms on the trailing edge (e.g., Parker, 1963; Sarabhai, 1963; Carovillano and Siscoe, 1969; Hundhausen, 1972). Because the pattern of

compression rotates with the Sun when the outflow from the Sun is time stationary, these high pressure regions are often called Corotating Interaction Regions (CIRs) (Smith and Wolfe, 1976). Here, we use the name, Stream Interaction Regions (SIRs), to include some transient and local stream interactions, which do not last even one rotation.

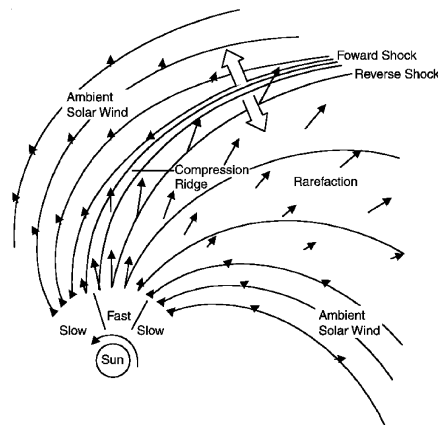


Figure 1. Schematic illustration of stream interaction near the solar equatorial plane in the inner heliosphere (after Pizzo, 1978).

The interaction between fast and slow solar wind begins in the inner heliosphere. SIRs thus are commonly well formed at Earth's orbit, 1AU from the Sun. The stream interfaces are distinguished as abrupt drops in particle density with simultaneous rises in proton temperature, and a large shear in the flow within SIRs (reviewed by Gosling and Pizzo, 1999). As the SIRs move farther away from the Sun, they eventually coalesce.

Magnetic field does not exert pressure along its length, but the magnetic field and plasma both contribute to the perpendicular pressure force. Since the dynamics of the solar wind structures is controlled by the total perpendicular pressure  $P_{\perp pp}$ ,  $B^2/2\mu_0 + nkT$ , and not by the constituents individually, we obtain simpler signatures in  $P_{\perp pp}$  than in the signatures of the constituent components. Moreover, irregularities in  $P_{\perp pp}$  are smoothed by compressional waves that radiate away inhomogeneities in pressure, leaving only sudden discontinuities caused by shocks. The peak pressure is

equal to the dynamic pressure of the flow on either side of the stream interface resolved along the normal to the boundary and in the reference frame of the boundary. Shocks arise when the change in velocity across the plasma interface exceeds the compressional wave speed so that linear waves can not act to transmit the pressure from the interaction into the surrounding plasma. At forward shocks, solar wind speed increases, while simultaneously proton number density and temperature both increase. At reverse shocks, solar wind speed still increases, while proton number density and temperature both decline. Sometimes, there is such a pair of shocks bounding a pressure enhancement region. Since the forces at the two sides of the SIR push in nearly opposite directions, the  $P_{\text{tpp}}$  peaks in the vicinity of the interface with gradual decreases on either side.

## 2. SIGNATURES OF SIRS

Assuming a constant solar wind electron temperature, 150,000 K, and a constant 4% alpha number fraction, we have calculated the total perpendicular pressure for the entire WIND solar wind data set (GSFC/MIT). Our criteria are mainly dependent on the behavior of  $P_{\text{tpp}}$  and are next most dependent on the solar wind speed (must be increasing). Other characteristics such as the compression of proton number density and magnetic field at the interface is approached, increased temperature at the interface and flow deflections gives additional assurance of the identification. We give some interesting examples herein.

Fig. 2 shows a SIR without shocks. The  $P_{\text{tpp}}$  profile is simple: an acceleration phase followed by a deceleration phase on an increasing speed profile. The components vary in a complex way. There is an irregular magnetic field, a constant thermal speed, and a density rise in the acceleration phase; and a sharp density drop at the interface; then the density and thermal speed both gradually decline in the deceleration phase.

Fig. 3 illustrates a SIR with the  $P_{\text{tpp}}$  enhancement bounded by a pair of forward-reverse shocks. The component variations are complex. The acceleration phase has temperature decrease while  $P_{\text{tpp}}$  increases; the deceleration phase has a declining temperature and density; magnetic field without rotations mimics  $P_{\text{tpp}}$ .

In Fig. 3, assuming the wave propagates in the direction perpendicular to the magnetic field, we find the fast magnetoacoustic wave speed to be 63 km/s at 00:33 UT on May 18th, and 82 km/s at 19:48 UT on May 18th. Using the minimum variance analysis, we can get the interface normal direction and then get the normal solar wind velocity jump is 114 km/s across 00:33 UT, and is 137 km/s across the jump at 19:48 UT. So the fast Mach numbers are 1.82 and 1.67 respectively at the two jumps. Thus these pressure jumps are consistent with the existence of the pair of forward-reverse shock.

## 3. VARIATION OF THE PROPERTIES OF SIRS DURING 1995-2003

Based on 1995-2003 WIND solar wind data, we have

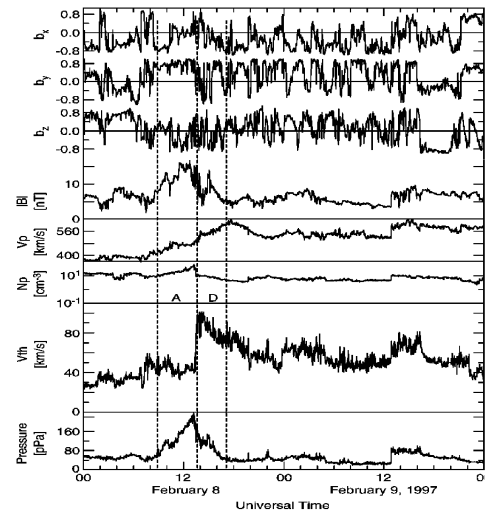


Figure 2. Stream interaction region without shocks. From top to bottom are shown the direction cosines of the magnetic field in GSM coordinates, the magnitude of the magnetic field, the solar wind speed, the proton density, the proton thermal speed and the total perpendicular pressure.

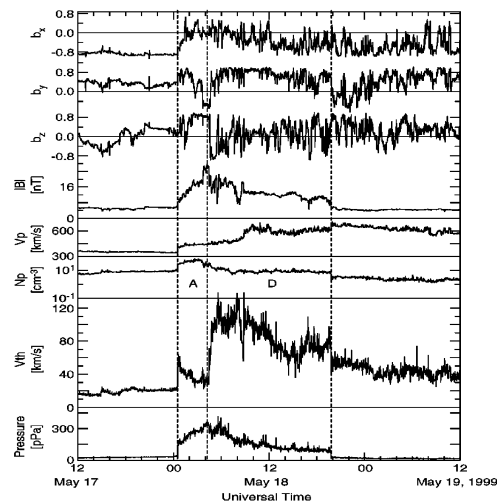
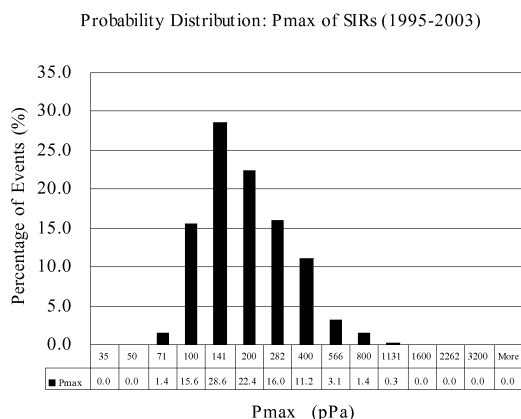


Figure 3. Stream interaction region bounded by shocks. See caption of Fig. 2.

identified 296 SIR events. Excluding data gaps and noisy data, the annual average SIR event number is about 33. We denote  $P_{\text{max}}$  as the peak of  $P_{\text{tpp}}$  and  $\Delta V$  as the change in the solar wind speed during each event. The two plots of Figure 4 and 5 show the probability



distribution of P<sub>max</sub> and  $\Delta V$  respectively. The P<sub>max</sub>

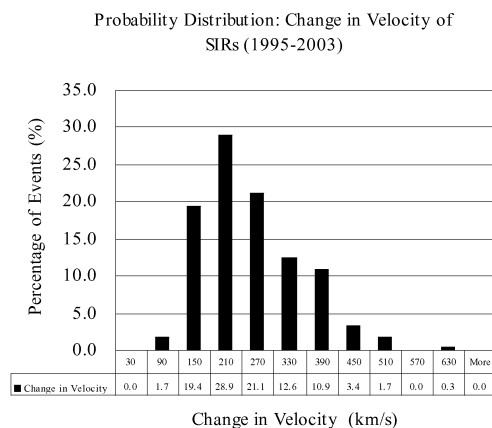
Figure 4. Probability distribution of the maximum total pressure for SIRs (WIND 1995-2003)

Table 1. SIR Statistics

Year	SIR #	% with Shock	<P <sub>max</sub> > ( $\delta$ P <sub>max</sub> )	< $\Delta V$ > ( $\delta$ $\Delta V$ )
1995	32	59.4	241.88 (129.61)	283.22 (95.90)
1996	32	40.6	130.75 (47.81)	194.75 (55.21)
1997	35	34.3	139.33 (46.49)	161.67 (56.10)
1998	31	45.2	172.61 (73.08)	228.55 (84.00)
1999	32	37.5	215.53 (122.17)	254.78 (107.15)
2000	31	25.8	186.65 (117.91)	239.35 (98.61)
2001	32	37.5	180.78 (107.25)	219.91 (75.22)
2002	37	35.1	236.24 (138.03)	242.51 (99.38)
2003	34	29.4	189.12 (111.80)	263.44 (90.40)
All	296	38.2	188.82 (110.09)	232.16 (92.24)

distributes mostly around 141 pPa, although it can vary from 54 pPa up to 850 pPa. The  $\Delta V$  profile has a similar distribution, centered on 210 km/s, with a variation range 66 ~ 603 km/s. The statistics are shown in Figures 4 and 5.

Table 1 lists the number of SIR events, percentage of events with shocks, average P<sub>max</sub> as well as its standard deviation, average  $\Delta V$  as well as its standard deviation. Unexpectedly, the occurrence rate of SIRs is almost constant (around 33) during the 9 years, despite the variation in the solar magnetic configuration during the period under study. However, the percentage of events with shocks decreases slowly during the declining phase of the solar cycle. On average about 38.2% of SIRs are associated with shocks or shock-like



structures at 1 AU. This number is larger than the previously expected low occurrence rate of SIRs with Figure 5. Probability distribution of the change in velocity of SIRs (WIND 1995-2003)

shocks at 1 AU, where the magnetoacoustic wave speed is not low. In addition, the P<sub>max</sub> averaged over 296 events is  $189 \pm 6$  pPa, where the uncertainty is the probable error of the mean. The average  $\Delta V$  is  $232 \pm 5$  km/s, larger than the average  $\Delta V$  of ICMEs ( $165 \pm 8$  km/s), consistent with the SIRs role in the interaction of fast streams with slow streams.

#### 4. SOLAR WIND HEATING

The number flux of the solar wind,  $nV$ , is roughly constant so that  $n$  and  $V$  are anticorrelated. Moreover the proton temperature of the solar wind is positively correlated with the solar wind speed ( $T \sim V^{1/2}$ ). Thus  $n_p$  and  $T_p$  are anticorrelated. One should not take this correlation as implying that the exponent ( $\gamma$ ) in the equation of state is less than unity. This anticorrelation has nothing to do with the compression or expansion of the solar wind plasma under adiabatic conditions but rather with the variable conditions in the acceleration region. Newbury *et al.* (1997) have, in fact, used the narrow region around stream interaction interfaces where the density and temperature change due to the compression of the plasma to show that the solar wind protons have a  $\gamma$  of  $5/3$  as expected.

The examples shown here illustrate how stream interactions contribute to solar wind heating. Between the dashed lines in Fig. 2 we see the increase in density caused by the interaction increasing from both sides toward the center. The center dashed line marks the interface. This compression may also be responsible for some of the temperature variation on the hot side of the interface, but on the cool side any compressional heating in this example has not overcome the spatial variation. In Fig. 3 shocks bound the stream interaction region. At each shock there is a hot layer. The

temperature profile may in fact be a clue to how long ago the shock was formed. In both cases it may have been recently, as the hot region is narrow.

This brief survey shows that stream interactions do heat the solar wind. The heating is weak and confined to a narrow region near the stream interface if the interaction is subsonic. However if the interaction produces a shock then the heating region moves away from the interface and produces (usually) a stronger heating pulse. Variations in the temperature can occur without any evidence of compression or rarefaction. These may be due to varying conditions at the source.

## 5. CONCLUSIONS

Total perpendicular pressure  $P_{\perp}$  can simplify the identification of different types of interactions. A peak with gradual slopes on its two sides is the identifying feature in the pressure of Stream Interaction Region (SIR). From 1995 to 2003, the occurrence rate of SIRs varies little, with about 33 events per year. On average about 38% of SIRs are associated with shocks or shock-like structures. In addition, the average peak pressure  $P_{\max}$  is  $189 \pm 6$  pPa, and the average  $\Delta V$  is as large as  $232 \pm 5$  km/s. The relative constancy of the stream interactions over the solar cycle is somewhat surprising given the change in the configuration of the solar magnetic field over the course of the solar cycle.

Perpendicular pressure also provides a good context from which to study the heating of the solar wind plasma at stream interface. Near the interface there is some compressional heating. When shocks form, there is heating at the shock. The duration of the heating is clearly evident from the duration of the enhanced temperatures. Stream interactions do not add measurability to solar wind heating for subsonic interactions but when the interaction becomes supersonic, heating occurs at the shocks and can

become significant.

## ACKNOWLEDGEMENTS

We have used the WIND plasma and magnetic field data throughout. We thank the MIT and Goddard plasma team (A.J. Lazarus and K. Ogilvie) and the magnetometer team (R.P. Lepping) for making these data available.

## REFERENCES

- Carovillano R. L. and Siscoe G. L., Corotating Structure in the Solar Wind, *Sol. Phys.*, 8, 401-414, 1969.
- Gosling J. T. and Pizzo V. J., Formation and Evolution of Corotating Interaction Regions and Their Three Dimensional Structure, *Space Sci. Rev.*, Vol. 89, 21-52, 1999.
- Hundhausen A. J., *Coronal Expansion and Solar Wind*, Springer-Verlag, New York, 1972.
- Hundhausen A. J., An Interplanetary View of Coronal Holes, in J. B. Ziker (ed.), *Coronal Holes and High Speed Wind Streams*, Colorado Assoc. Univ. Press., Boulder, 225-329, 1977.
- Newbury J. A., Russell C. T. and Lindsay G. M., Solar Wind Polytopic Index in the Vicinity of Stream Interactions, *Geophys. Res. Lett.*, 24, 1431, 1997.
- Parker E. N., *Interplanetary Dynamical Processes*, John Wiley, New York, 1963.
- Pizzo V. J., A Three-Dimensional Model of Corotating Streams in the Solar Wind - I. Theoretical Foundations, *J. Geophys. Res.*, 83, 5563-5572, 1978.
- Sarabhai V., Some Consequences of Nonuniformity of Solar-Wind Velocity, *J. Geophys. Res.*, 68., 1555-1557, 1963.
- Smith E. J. and Wolfe J. H., Observations of Interaction Regions and Corotating Shocks between One and Five AU: Pioneers 10 and 11, *J. Geophys. Res.*, 3, 137-140, 1976.